Electrocatalysis (2020) 11:555–566
https://doi.org/10.1007/s12678-020-00615-w

ORIGINAL RESEARCH

Evaluating the Effect of WO_3 on Electrochemical and Corrosion Properties of TiO_2-RuO_2-Coated Titanium Anodes with Low Content of RuO_2

Elzbieta Kusmierek[1]

Published online: 27 June 2020

Abstract
The electrochemical and corrosion characterization of $Ti_{0.97}Ru_{0.03}O_2$/Ti electrodes modified with WO_3 was reported. Modification of $Ti_{0.97}Ru_{0.03}O_2$/Ti electrodes with WO_3 was previously described as improving the effectiveness of an azo dye degradation in a photoelectrochemical treatment. Thus, the effect of WO_3 introduction to oxide film on electrode surface on electrochemical behaviour and stability of the modified electrodes was investigated. Moreover, corrosion behaviour of $Ti_{0.97}Ru_{0.03}O_2$/Ti electrodes modified with WO_3 was evaluated with the application of potentiodynamic polarization sweep method and open circuit potential measurement. Electrodes modified with WO_3 revealed higher anodic and cathodic peak currents in $K_4[Fe(CN)_6]$ solution (by 35% for 6%WO_3 content) indicating higher electroactive surface area and faster electron transfer reaction. An increase in WO_3 amount in the oxide layer caused an increase in the number of active sites determined in Na_2SO_4 and most of them (more than 80%) were located in the outer and more accessible surface. The investigation of the tested electrodes at high potentials at which oxygen evolution is observed, allowed their classification in the following order showing an increase in their activity towards oxygen evolution reaction: $Ti_{0.97}Ru_{0.03}O_2$/Ti < $Ti_{0.94}Ru_{0.03}O_2$-$W_{0.03}O_3$/Ti < $Ti_{0.91}Ru_{0.03}O_2$-$W_{0.06}O_3$/Ti. Although the electrode modification with WO_3 resulted in lower resistance to corrosion in Na_2SO_4 solution regarding corrosion potential, corrosion current densities were clearly lower in comparison with the non-modified electrode, especially after longer immersion in the solution. ASTs showed that even a small addition of WO_3 increased the lifetime of the electrodes. The $Ti_{0.97}Ru_{0.03}O_2$/Ti electrode modification with WO_3 seemed to be advantageous for their application in electrochemical and photoelectrochemical degradation of organic pollutants.

Keywords Anode material · Electrochemistry · Active surface · Corrosion · Stability

Introduction

In recent years, the investigation of electrocatalytic and corrosion properties of oxide electrodes has received considerable attention [1–9]. Metal oxide–coated titanium electrodes are called DSAs (dimensionally stable anodes) and are the most important electrodes in electrochemical engineering due to their electrocatalytic properties and stability [10, 11]. DSA-type electrodes are widely used in many fields of electrochemistry such as chlorine production, electroplating and metal electrowinning, cathodic protection, water electrolysis and wastewater treatment [10, 12–18]. TiO_2-RuO_2/Ti electrodes are typical DSAs which are commonly applied in the oxidation of organic compounds which occurs with simultaneous evolution of oxygen. However, the oxide electrodes applied in electrochemical industry have some limitations including a limited service lifetime [10, 19]. RuO_2 is a metallic oxide and exhibits good activity in oxygen evolution reaction (OER) and chlorine evolution reaction (ClER). This metal oxide ensures proper electric conductivity but is unstable under oxygen evolution reaction due to concurrent reaction of its dissolution [20]. TiO_2 is a semiconductor generally regarded as the most effective photoinduced catalyst and commonly applied in oxidation of organic and inorganic pollutants in air and water [21, 22]. Moreover, the electrodes containing TiO_2 in the oxide layer can be also applied in photoelectrochemical treatment of organic pollutants [23].

✉ Elzbieta Kusmierek
elzbieta.kusmierek@p.lodz.pl

1 Institute of General and Ecological Chemistry, Lodz University of Technology, ul. Zeromskiego 116, 90-924 Lodz, Poland

The application of mixed oxides containing more than two components can improve not only electrocatalytic properties of an electrode material but also its stability. Introduction of the third metal oxide which is a semiconductor with a bandgap which enables its photoexcitation with irradiation from VIS region can improve the efficiency of a photoelectrochemical degradation of organic pollutants and enable application of an irradiation with lower wavelengths. Thus, in the previous paper [24], we suggested modification of TiO_2-RuO_2/Ti electrodes by introduction of WO_3 to the oxide layer.

WO_3 is characterized by a bandgap of 2.6 eV, which is about 0.6 eV narrower than TiO_2 bandgap, and makes it capable of being excited by visible light [25]. Moreover, its high stability in acidic solutions, resistance to photocorrosion and high conductivity is also important when it is applied in the treatment of wastewater contaminated by organic pollutants, especially acids [26, 27]. Thus, it seems to be purposeful to couple WO_3 with other semiconductors, i.e. TiO_2, ZnO, $BiVO_4$ [28–30]. WO_3 can be also applied in photocatalytic water splitting to produce hydrogen gas simultaneously with organic pollutant degradation using visible solar light [28, 31, 32]. The addition of WO_3 to TiO_2 results in an increase in photoelectrocatalytic activity of the electrodes applied in the degradation of organic pollutants present in industrial wastewater [28, 32–34]. The contribution of WO_3 in enhanced photoelectroacatalytic activity can be explained by increased surface adsorption affinity and improved charge carrier separation. However, an excessive amount of WO_3 sometimes does not enhance the activity of the electrodes due to the transition of W^{6+}/W^{5+} [27].

These electrodes are exposed to corrosive media, i.e. industrial wastewater. As the result of corrosion or dissolution, some properties of the oxide film on electrode surface can change [35]. Thus, it is important to determine an effect of WO_3 incorporation to the oxide film on corrosion characterization and stability of the modified electrodes. The effect of the electrode modification by WO_3 addition on OER should also be investigated. The OER accounts for a large part of overpotential in the case of semiconductors [36], and its investigation is important in searching for efficient photoanodes.

The composition and properties of active compounds in the oxide film at the electrode surface strongly affect the properties of the electrode material taking into consideration not only its electrochemical and corrosion characterization but also its stability. The electrode stability can be evaluated by accelerated stability tests (ASTs). The electrochemical activity of electrodes is related to the development of their surface and an increase in the number of active centres [37]. Changes in the electroactive surface area (EAS) caused by electrode modification can be determined based on voltammetric determination [38–41] which enables monitoring of the surface of the oxide electrodes. However, the surface charging of oxide electrodes, particularly semiconductor metallic oxides, is complex. This depends on the supporting electrolyte and the acid/base surface properties of the oxides related to proton injection/ejection process including the solid-state surface redox transitions (SSSRTs) [42, 43].

In the recent paper [44], the results of electrochemical and corrosion investigations of the electrodes with higher content of RuO_2 and modified with WO_3, i.e. $Ti_{0.7\text{-}x}Ru_{0.3}O_2$-$W_xO_3$/Ti electrodes, were presented. In this paper, the results of detailed electrochemical and corrosion properties of the electrodes with lower content of RuO_2 and modified with WO_3, i.e. $Ti_{0.97\text{-}x}Ru_{0.03}O_2$-$W_xO_3$/Ti electrodes, are reported. The results of the experiments are compared with the non-modified electrode in order to determine an effect of WO_3.

Experimental

Chemicals and Materials

Electrochemical measurements were carried out in solutions of $K_4[Fe(CN)_6]$ (5 mM) prepared by dissolving hexacyanoferrate(II) trihydrate ($K_4[Fe(CN)_6]\cdot 3H_2O$, Merck) in 0.1 M KCl, and in the solution of Na_2SO_4 at the concentration of 0.1 M. Double distilled water was used in preparation of all solutions and throughout all experiments. All the chemicals applied in experiments were of analytical grade.

$Ti_{0.97\text{-}x}Ru_{0.03}O_2$-$W_xO_3$/Ti ($x = 0$, 0.03, 0.06) was prepared according to the procedure described in the paper [44]. The nominal compositions of the coatings were achieved by properly adjusted concentrations of chloride precursor mixtures in *n*-butanol. The content of TiO_2 was changed according to the amount of WO_3 introduced to the oxide layer while RuO_2 content was constant in order to ensure the electrical conductivity and catalytic activity of the tested anodes. The geometric surface area of the tested electrodes exposed to solutions was the same and totalled 2 cm^2. The non-modified electrode, i.e. $Ti_{0.97}Ru_{0.03}O_2$/Ti was applied in electrochemical measurements in order to compare results obtained for the modified electrodes.

Characterization of Electrodes

Electrochemical and corrosion measurements were carried out in the three-electrode cell connected to the electrochemical workstation—μAutolab III (Metrohm Autolab B.V., The Netherlands). The cyclic voltammetry method was applied in recording curves presenting a dependence of current vs. potential. Voltammetric curves were analysed with the application of Nova software vs. 2.1. Platinum electrode was used as a counter electrode. The potential of the working electrode was measured vs. saturated calomel electrode (SCE) in all measurements.

Cyclic voltammograms were recorded in solutions with a volume of 20 mL at different scan rates in the range from 2 to 500 mV s^{-1}. Before measurements, dissolved oxygen was removed from solutions by purging them with argon for at least 20 min. Argon blanket was kept over solution surface during measurements in order to prevent oxygen diffusion to the bulk solution. Voltammetric measurements were performed at least thrice.

Corrosion properties of the tested electrodes were determined in Na_2SO_4 solution and were evaluated using electrochemical techniques such as open circuit potential (OCP) measurement followed by potentiodynamic polarization sweep. The potential of a tested electrode was measured as a function of time in order to determine the OCP value after its immersion in a solution. The OCP measurement was performed by 1 h or was stopped earlier when its value was established (dE/dt ≤ 1 μV s^{-1}). Next, the tested electrodes were polarized in the potential range of OCP ± 200 mV. Linear polarization curves were recorded with the scan rate of 2 mV s^{-1}.

Additionally, an electrode stability was assessed in accelerated stability tests (ASTs) carried out in Na_2SO_4 solution and in a three-electrode cell at room temperature. Measurements were performed at a constant current density of 0.2 A cm^{-2} supplied by a potentiostat/galvanostat Autolab PGSTAT 302N (Metrohm Autolab B.V.). The lifetime of the tested electrodes was evaluated as the electrolysis time at which the anodic potential exceeded the value of at least 2 V higher than its initial value recorded at time zero.

The morphological characteristics of all tested electrodes were investigated using S-4700 Hitachi (Japan) scanning electron microscope. SEM micrographs were obtained at a magnification of ×10,000, scale bar 5.00 μm.

Results and Discussion

Cyclic Voltammetry Study in Ferrocyanide Solution

Cyclic voltammetry (CV) in $K_4[Fe(CN)_6]$ solution was applied in the investigation of the electrochemical properties of $Ti_{0.97\text{-}x}Ru_{0.03}O_2\text{-}W_xO_3/Ti$ electrodes. The exemplary cyclic voltammograms recorded at the scan rate (v) of 5 mV s^{-1} for the tested electrodes are presented in Fig. 1. Electrochemical parameters characterizing $[Fe(CN)_6]^{3-}/[Fe(CN)_6]^{4-}$ redox system are listed in Table 1.

The modification of $Ti_{0.97}Ru_{0.03}O_2/Ti$ electrodes by introduction of WO_3 to the oxide layer in their surface results in an increase of the anodic and cathodic peak currents (by about 35% for the electrode with 6%WO_3). The anodic and cathodic current ratio is almost the same for all tested electrodes and very close to 1, which indicates the reversible character of the redox couple. WO_3 does not influence the half-wave potential

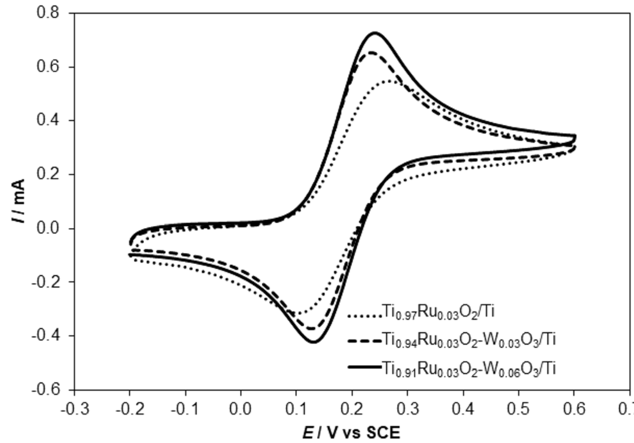

Fig. 1 CV curves recorded at $Ti_{0.97\text{-}x}Ru_{0.03}O_2\text{-}W_xO_3/Ti$ electrodes in $K_4[Fe(CN)_6]$ solution (5 mM in 0.1 M KCl); $v = 5$ mV s^{-1}

$E_{1/2}$ determined from the anodic (E_{pa}) and cathodic (E_{pc}) peak potentials by using the expression $(E_{pa} + E_{pc})/2$. However, the peak-to-peak separation (ΔE_p) is lower by 56 mV while the content of WO_3 in the oxide layer is 3 and 6%. ΔE_p is directly correlated to the electron transfer kinetics and indicates that the electrode modification with WO_3 results in more reversible electron transfer in the electrochemical reaction. Moreover, electrochemical parameters presented in Table 1 (I_{pa} and I_{pc}) also indicate the faster electron transfer reaction at the modified electrodes.

In order to determine and compare electroactive surface area (EAS) of the tested electrodes, cyclic voltammograms were recorded at the tested electrodes at various scan rates. The Randles-Sevcik equation [38, 45] often applied for the determination of EAS can be used in the case of all electrochemical processes which are controlled by diffusion. Thus, dependences of peak current (I_p) on the square root of the scan rate (v) were determined and are presented in Fig. 2.

These dependences are linear in the case of all tested electrodes and prove a diffusion-controlled process. The dependence for the non-modified electrode ($Ti_{0.97}Ru_{0.03}O_2/Ti$) is presented only in the scan rate range from 2 to 100 mV s^{-1} since anodic and cathodic peaks were poorly shaped in curves recorded at higher scan rates. Moreover, the diffusion control of the process was confirmed by dependences of $\log I_p$ vs. $\log v$ determined for anodic and cathodic peaks. The equations describing these dependences are presented in Table 2.

The linear dependences of $\log I_p$ vs. $\log v$ are characterized by an experimental slope of 0.38–0.40 for the anodic peaks and 0.37–0.42 for the cathodic peaks. These values are lower than 0.5 which is expected theoretically for the $\log I_p$ vs. $\log v$ plots under diffusion control. This is probably due to the existence of a kinetic contribution to the reaction control [46, 47]. Moreover, an increase in the scan rate results in significant increase in the value of ΔE_p (0.560 V at 0.5 V s^{-1}), indicating more irreversible electron transfer electrochemical reaction. Taking these into consideration, determination of

Table 1 CV parameters determined for $Ti_{0.97-x}Ru_{0.03}O_2$-W_xO_3/Ti electrodes (I_p—peak current, E_p—peak potential, ΔE_p—difference between anodic and cathodic peak potential, $E_{1/2}$—half-wave potential) from CV curves presented in Fig. 1

Electrode	E_{pa} (V)	I_{pa} (mA)	E_{pc} (V)	I_{pc} (mA)	I_{pa}/I_{pc}	ΔE_p (V)	$E_{1/2}$ (V)
$Ti_{0.97}Ru_{0.03}O_2$/Ti	0.268	0.516	0.103	− 0.498	1.04	0.165	0.186
$Ti_{0.94}Ru_{0.03}O_2$-$W_{0.03}O_3$/Ti	0.236	0.644	0.127	− 0.600	1.07	0.109	0.182
$Ti_{0.91}Ru_{0.03}O_2$-$W_{0.06}O_3$/Ti	0.240	0.709	0.131	− 0.666	1.06	0.109	0.186

EAS calculated using the above mentioned Randles-Sevcik equation was not performed because it could result in incorrect EAS values. However, it can be predicted that the EAS values for the modified electrodes should be higher than the EAS value for the non-modified electrode, and the higher content of WO_3 should also result in higher EAS. Thus, EAS was also evaluated by determination of number of electroactive sites on the surface of the tested electrodes and is presented in the next section.

The results of the electrochemical characterization of $Ti_{0.97-x}Ru_{0.03}O_2$-W_xO_3/Ti electrodes were also compared with the results obtained for $Ti_{0.7-x}Ru_{0.3}O_2$-W_xO_3/Ti electrodes which were described in the paper [44]. The electrochemical reaction observed in $K_4[Fe(CN)_6]$ solution is more irreversible in the case of $Ti_{0.97-x}Ru_{0.03}O_2$-W_xO_3/Ti. The electrode modification with WO_3 causes an increase in reversibility of the process in comparison with the non-modified electrode in contrary to $Ti_{0.7-x}Ru_{0.3}O_2$-W_xO_3/Ti electrodes. Moreover, the higher content of WO_3 in $Ti_{0.97-x}Ru_{0.03}O_2$-W_xO_3/Ti results in higher values of I_{pa} and I_{pc} also in contrary to $Ti_{0.7-x}Ru_{0.3}O_2$-W_xO_3/Ti electrodes. It can be concluded that the introduction of WO_3 to $Ti_{0.97}Ru_{0.3}O_2$/Ti electrode results in higher reaction rate. The opposite conclusion was drawn in the case of $Ti_{0.7}Ru_{0.3}O_2$/Ti modified with WO_3.

The tested electrodes were also applied in electrochemical degradation of an azo dye (Acid Orange 7) described in the paper [24]. The highest value of the dye oxidation current determined at the specified potential in the CV curves was observed at $Ti_{0.91}Ru_{0.03}O_2$-$W_{0.06}O_3$/Ti electrode and was only slightly lower than in the case of electrodes with higher content of RuO_2. Moreover, the degradation of the dye observed in the electrochemical process was also the highest at $Ti_{0.91}Ru_{0.03}O_2$-$W_{0.06}O_3$/Ti electrode, taking into consideration the dye conversion calculated as a change in chemical oxygen demand (COD) and total organic carbon (TOC). This proves purposefulness of $Ti_{0.97}Ru_{0.03}O_2$/Ti electrode modification with WO_3.

Cyclic Voltammetry Study in Na_2SO_4 Solution

The electrochemical properties of $Ti_{0.97-x}Ru_{0.03}O_2$-W_xO_3/Ti electrodes were also investigated in Na_2SO_4 solution which can be applied as the supporting electrolyte in electrochemical and photoelectrochemical degradation of organic compounds, especially dyes [23]. CV curves were recorded at the tested electrodes with various scan rates. The voltammetric charge determined from a cyclic voltammetry curve recorded in the potential range between hydrogen and oxygen evolution has been found to be proportional to EAS and has been attributed to the number of electrochemically active sites on the electrode surface [40, 41]. The voltammograms recorded at the tested electrodes reveal the rectangular shape with the

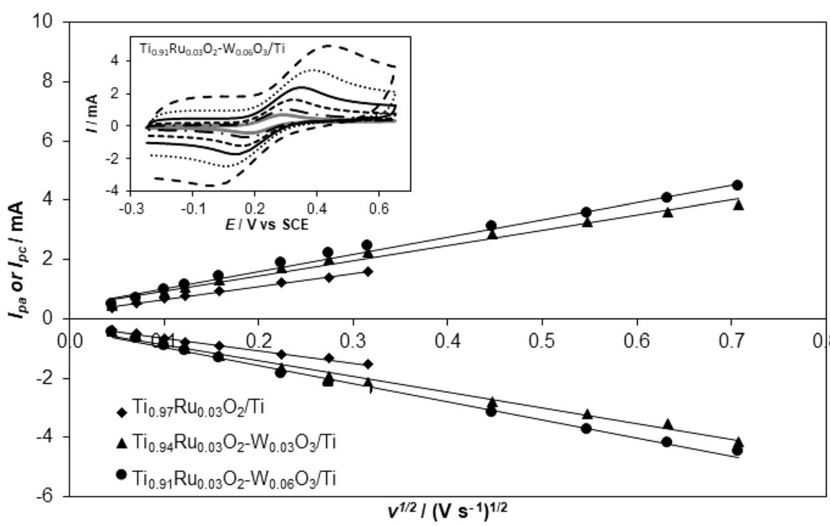

Fig. 2 Dependence of I_{pa} and I_{pc} vs. $v^{1/2}$ for $Ti_{0.97-x}Ru_{0.03}O_2$-W_xO_3/Ti electrodes, determined in $K_4[Fe(CN)_6]$ solution (5 mM in 0.1 M KCl) at various scan rates between 2 and 500 mV s^{-1}. Inset: CV curves recorded at $Ti_{0.91}Ru_{0.03}O_2$-$W_{0.06}O_3$/Ti electrode at various scan rates

Table 2 The equations presenting linear dependences of $\log I_p$ vs. $\log v$ determined for $Ti_{0.97\text{-}x}Ru_{0.03}O_2\text{-}W_xO_3/Ti$ electrodes in $K_4[Fe(CN)_6]$ (5 mM in 0.1 M KCl)

Electrode	Equation	R^2
Anodic peak		
$Ti_{0.97}Ru_{0.03}O_2/Ti$	$y = 0.375x + 0.573$	0.9997
$Ti_{0.94}Ru_{0.03}O_2\text{-}W_{0.03}O_3/Ti$	$y = 0.396x + 0.731$	0.9966
$Ti_{0.91}Ru_{0.03}O_2\text{-}W_{0.06}O_3/Ti$	$y = 0.399x + 0.778$	0.9976
Cathodic peak		
$Ti_{0.97}Ru_{0.03}O_2/Ti$	$y = 0.367x + 0.552$	0.9985
$Ti_{0.94}Ru_{0.03}O_2\text{-}W_{0.03}O_3/Ti$	$y = 0.408x + 0.733$	0.9982
$Ti_{0.91}Ru_{0.03}O_2\text{-}W_{0.06}O_3/Ti$	$y = 0.418x + 0.795$	0.9989

increasing scan rate, indicating a pseudo-capacitive behaviour. However, some differences between $Ti_{0.97}Ru_{0.03}O_2/Ti$ electrode and the electrodes modified with WO_3 are observed. In the case of the non-modified electrode, the cyclic voltammogram is similar to the voltammogram recorded for $Ti_{0.7}Ru_{0.3}O_2/Ti$ electrode in the same solution [44]. Scarcely visible one pair of anodic and cathodic peak probably corresponds to the redox transition between Ru(III) and Ru(IV). The pseudo-capacitive character of this electrode can result from the solid-state surface redox transitions (SSSRT) of ruthenium species related to proton exchange reaction [42]. However, these peaks are not observed at CV curves recorded at the modified electrodes. In the case of $Ti_{0.97\text{-}x}Ru_{0.03}O_2\text{-}W_xO_3/Ti$ electrodes, a pair of anodic and cathodic peaks appears at lower potentials (about 0.2 V). As these peaks were not observed at the non-modified electrode, it can be predicted that they are attributed to the change of transition state between W(VI) and W(V) [48–50] according to the following reaction [51, 52]:

$$WO_3 + xH^+ + xe^- \leftrightarrow H_xWO_3 \quad (1)$$

and resulting in the formation of hydrogen tungsten bronzes.

In contrary to $Ti_{0.7\text{-}x}Ru_{0.3}O_2\text{-}W_xO_3/Ti$ electrodes [44], not only change in the CV curves was observed but also the current values observed for $Ti_{0.97\text{-}x}Ru_{0.03}O_2\text{-}W_xO_3/Ti$ electrodes were clearly higher than those observed for the non-modified electrode. The higher content of WO_3 in the oxide film resulted in higher current in the CV curves. This can be attributed to an increase in the number of active sites contributing to SSSRT. In order to prove the increase in active site number, the cyclic voltammograms were recorded in Na_2SO_4 electrolyte, with various scan rates in the range from 5 to 500 mV s^{-1}. If voltammetry charge is determined in a potential range where hydrogen and oxygen is not evolved, then it can be applied in estimation of EAS according to the procedure described in the paper [44]. The reversibility of the pseudo-capacitance process, and dependences of $1/q^* = f(v^{1/2})$ and $q^* = f(v^{-1/2})$ obtained for the tested electrodes are presented in Figs. 3 and 4. The results of total, inner and outer charge calculations are shown in Table 3.

The ratio of anodic to cathodic charge (q^*_a/q^*_c) indicating the reversibility of the redox process, slightly exceeds 1 in the case of the tested electrodes and indicates almost reversible behaviour of the solid-state surface redox transitions. The lowest value of q^*_a/q^*_c was observed in the case of the electrode modified with 6% WO_3. This can be explained by higher electro-negativity of W than Ru, and by the fact that WO_3 is more acidic than RuO_2, assuming that the rise in capacitive performance results from proton exchange between the catalyst surface and the electrolyte. If the electrode is modified by 6% WO_3 which is more acidic than RuO_2, then the SSSRT become more reversible.

Figure 4 and Table 3 prove that modification of $Ti_{0.97}Ru_{0.03}O_2/Ti$ electrodes with WO_3 increases the number of active surface sites by 19% (3%WO_3) and 46% (6%WO_3) in comparison with the non-modified electrode. Moreover, $Ti_{0.94}Ru_{0.03}O_2\text{-}W_{0.03}O_3/Ti$ and $Ti_{0.91}Ru_{0.03}O_2\text{-}W_{0.06}O_3/Ti$ electrodes exhibit slightly lower values of q^*_{out}/q^*_{tot} ratio than the non-modified one, which indicate that most of the active sites are more accessible. In the case of $Ti_{0.91}Ru_{0.03}O_2\text{-}W_{0.06}O_3/Ti$ electrode, 88% of the voltammetric charge is associated with outer and more accessible active sites, while 12% of the voltammetric charge is due to the inner and less accessible active sites located in pores. That electrode should be the most active in the electrochemical degradation of organic compounds taking into consideration its highest number of outer active sites on the electrode surface in comparison with the non-modified electrode and the electrode modified with 3% WO_3. Similar values of q^*_{out}/q^*_{tot} and q^*_{in}/q^*_{tot} calculated for the electrodes with 3 and 6% WO_3 in their oxide layers indicate the similarity of their surface morphology. Figure 5 shows some representative SEM micrograph of $Ti_{0.97\text{-}x}Ru_{0.03}O_2\text{-}W_xO_3/Ti$ electrodes. The non-modified

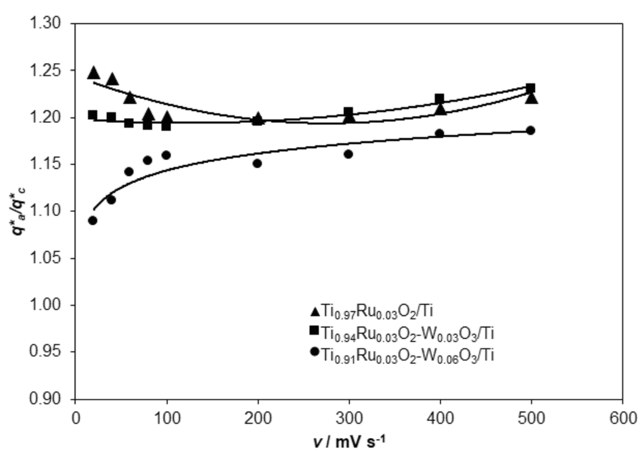

Fig. 3 A dependence of q^*_a/q^*_c vs. scan rate (v) used in estimation of the pseudo-capacitance process reversibility for $Ti_{0.97\text{-}x}Ru_{0.03}O_2\text{-}W_xO_3/Ti$ electrodes

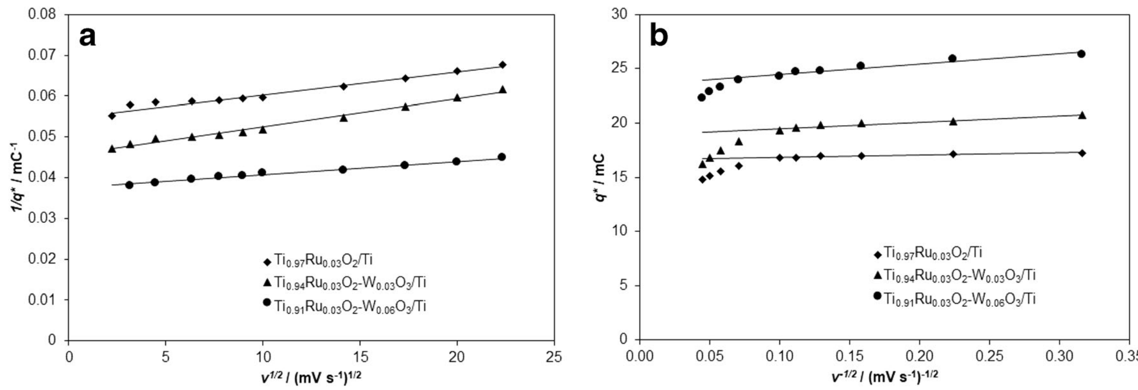

Fig. 4 Dependences of $1/q^*$ vs. $v^{1/2}$ (**a**) and q^* vs. $v^{-1/2}$ (**b**) determined for $Ti_{0.97\text{-}x}Ru_{0.03}O_2\text{-}W_xO_3/Ti$ electrodes in 0.1 M Na_2SO_4

electrode ($Ti_{0.97}Ru_{0.03}O_2/Ti$) reveals "mud" structure with some micrometre cracks. The cracks can result from the solvent evaporation during electrode preparation. Much less cracks, which are narrower, are observed in the case of the electrode modified with 3% WO_3. Probably, WO_3 covers some cracks. In the case of the electrode modified with twice higher amount of WO_3 (6%), cracks are scarcely visible and some excessive amounts of WO_3 exist as micrometre random deposits overlaying the electrode surface with cracks.

The value of q^*_{in}/q^*_{tot} ratio can be used in estimation of electrode porosity [53]. The tested electrodes reveal relatively low and comparable porosity (Table 3). But this factor is slightly higher for $Ti_{0.94}Ru_{0.03}O_2\text{-}W_{0.03}O_3/Ti$ in comparison with $Ti_{0.67}Ru_{0.3}O_2\text{-}W_{0.03}O_3/Ti$ electrode [44]. The results of the investigation prove that the modification of $Ti_{0.97}Ru_{0.03}O_2/Ti$ electrodes with WO_3 has a significant impact on the electroactive surface area. The number of active sites increases with an increase of WO_3 amount in the oxide film on the electrode surface. They are mainly (more than 80%) located at the outer and more accessible surface of the electrodes. Taking into consideration the previous results described in the paper [24], the electrooxidation currents of the azo dye observed at the voltammograms recorded at the tested electrodes and determined at the specified potential (0.8 V vs. SCE) were also higher than at the non-modified electrode. This is in accordance with higher number of active sites at the surface of the modified electrodes. Moreover, the electrochemical degradation of the azo dye was more efficient at the modified electrodes taking into consideration not only discoloration but also mineralisation expressed as a decrease in chemical oxygen demand (COD) and total organic carbon (TOC).

Anodic Polarization Curves—Oxygen Evolution

The behaviour of electrode materials at high potentials is interesting in studies on the treatment of recalcitrant organic pollutants by electrochemical methods. Oxygen evolution reaction (OER) is one of the most important electrochemical processes occurring simultaneously with the electrochemical oxidation of organic compounds. Thus, OER was investigated on the tested electrodes. Figure 6 presents representative anodic polarization curves recorded in 0.1 M Na_2SO_4 solution in the potential range to 1.4 V and with the scan rate of 5 mV s^{-1}. Taking into consideration that voltammetric charge is related to EAS and changes for modified and non-modified electrodes, the measured currents in the polarization curves were normalized with the respect to outer charge (Table 3) in order to describe true electrocatalytic effects.

The comparison of the electrocatalytic properties of electrode materials can be based on exchange current density determined at specified potential and Tafel slope which is related to reaction mechanism. High current densities and low Tafel slopes indicate an electrocatalyst characterized by high activity [9, 43]. Differences in exchange current densities related to OER observed at $Ti_{0.97\text{-}x}Ru_{0.03}O_2\text{-}W_xO_3/Ti$ electrodes are presented in Fig. 6. The activity of these electrodes can be compared based on potential values determined at the specified current density. The potential values at 0.068 mA mC^{-1} show a decrease in the activity of the electrodes in the following order: $Ti_{0.91}Ru_{0.03}O_2\text{-}W_{0.06}O_3/Ti$ (1.339 V) > $Ti_{0.94}Ru_{0.03}O_2\text{-}W_{0.03}O_3/Ti$ (1.357 V) > $Ti_{0.97}Ru_{0.03}O_2/Ti$ (1.400 V). This is quite an opposite order in comparison with the activity order presented for the $Ti_{0.7\text{-}x}Ru_{0.3}O_2\text{-}W_xO_3/Ti$

Table 3 The values of total (q^*_{tot}), outer (q^*_{out}) and inner (q^*_{in}) charges determined for $Ti_{0.97\text{-}x}Ru_{0.03}O_2\text{-}W_xO_3/Ti$ electrodes from CV curves recorded in 0.1 M Na_2SO_4 at different scan rates

Electrode	q^*_{tot} (mC)	q^*_{out} (mC)	q^*_{out}/q^*_{tot}	q^*_{in}/q^*_{tot}
$Ti_{0.97}Ru_{0.03}O_2/Ti$	18.36	16.63	0.91	0.09
$Ti_{0.94}Ru_{0.03}O_2\text{-}W_{0.03}O_3/Ti$	21.93	18.92	0.86	0.14
$Ti_{0.91}Ru_{0.03}O_2\text{-}W_{0.06}O_3/Ti$	26.76	23.50	0.88	0.12

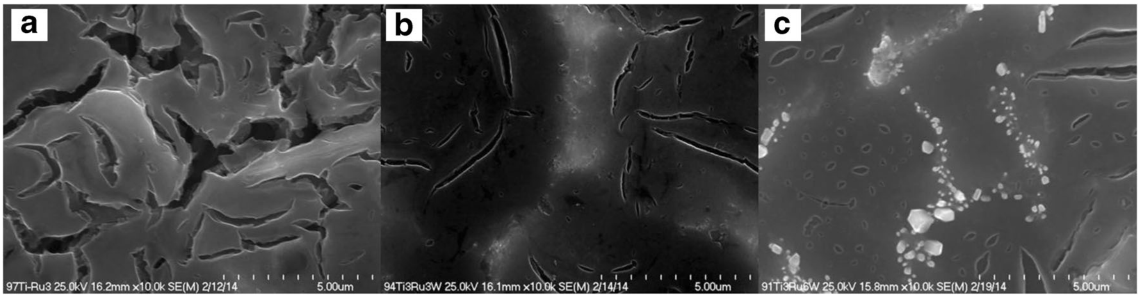

Fig. 5 SEM microphotographs of $Ti_{0.97}Ru_{0.03}O_2$/Ti (**a**), $Ti_{0.94}Ru_{0.03}O_2$-$W_{0.03}O_3$/Ti (**b**) and $Ti_{0.91}Ru_{0.03}O_2$-$W_{0.06}O_3$/Ti (**c**) electrodes

electrodes. If RuO_2 content in the oxide layer was higher (30%), then the highest activity of the electrode material was observed in the case of the non-modified one [44]. This can be related to different acid-base properties of the electrodes with higher (30%) and lower (3%) contents of RuO_2 in the oxide layer of the electrode surface and an effect of the modification with WO_3.

Tafel plots determined for OER observed at $Ti_{0.97-x}Ru_{0.03}O_2$-W_xO_3/Ti electrodes (Fig. 6) are similar and indicate the same reaction mechanism. However, especially in the case of $Ti_{0.91}Ru_{0.03}O_2$-$W_{0.06}O_3$/Ti electrode, slight deviation from Tafel line can be noticed at higher current densities. This deviation can result from a change in a Tafel slope (change in reaction mechanism) or from uncompensated ohmic drop. Thus, Tafel plots were corrected in the case of all tested electrodes, according to the procedure described in the paper [54] and applied in the previous investigation [44]. After IR-compensation, the Tafel plots revealed only one slope in the case of $Ti_{0.97-x}Ru_{0.03}O_2$-W_xO_3/Ti electrodes. OER generally proceeds in three steps in acidic and alkaline media [44, 54, 55]. The rate determining step (rds) for an electrode corresponds to its Tafel slope of OER and depends on strength of the adsorption of intermediates, which in turn depends on the composition of the oxide layer [55]. In the case of the supporting electrolyte (0.1 M Na_2SO_4) applied in the investigation described in this paper, IR-compensated Tafel plots are characterized by the following slope values: 220.2 mV dec^{-1} ($Ti_{0.97}Ru_{0.03}O_2$/Ti), 223.3 mV dec^{-1} ($Ti_{0.94}Ru_{0.03}O_2$-$W_{0.03}O_3$/Ti) and 194.1 mV dec^{-1} ($Ti_{0.91}Ru_{0.03}O_2$-$W_{0.06}O_3$/Ti).

$Ti_{0.97-x}Ru_{0.03}O_2$-W_xO_3/Ti electrodes reveal relatively high Tafel slopes, higher than 120 mV dec^{-1} which can result from the non-stoichiometry of the oxides at electrode surface and the number of sites to absorb the hydroxyl ions from water [56]. These values are also higher than Tafel slopes determined for $Ti_{0.7-x}Ru_{0.3}O_2$-W_xO_3/Ti by 30–60 mV and prove their lower activity. Moreover, the values of Tafel slope b indicate that the first step of OER including the formation and adsorption of the first intermediate S–OH_{ads} is the rds. Before oxygen evolution occurs at a catalytic oxide electrode, the hydroxyl radicals are first adsorbed at the active sites of the electrode. If the number of active sites to absorb the hydroxyl ions from water increases, oxygen evolution occurs more easily and the Tafel slope lowers. The highest current intensity and the lowest Tafel slope are observed in the case of $Ti_{0.91}Ru_{0.03}O_2$-$W_{0.06}O_3$/Ti electrode, indicating good electrocatalytic properties of the oxide film at the electrode surface.

The obtained results show that the electrodes modified with WO_3 reveal higher activity towards OER. The electrode with 6% WO_3 seems to be more active than the electrode with 3% WO_3. Moreover, the application of $Ti_{0.91}Ru_{0.03}O_2$-$W_{0.06}O_3$/Ti electrode in electrochemical and photoelectrochemical degradation of the azo dye described in the paper [24] resulted in the highest efficiency of the dye degradation calculated as a change in TOC and COD, in comparison with the electrode modified with 3% WO_3 and the non-modified one.

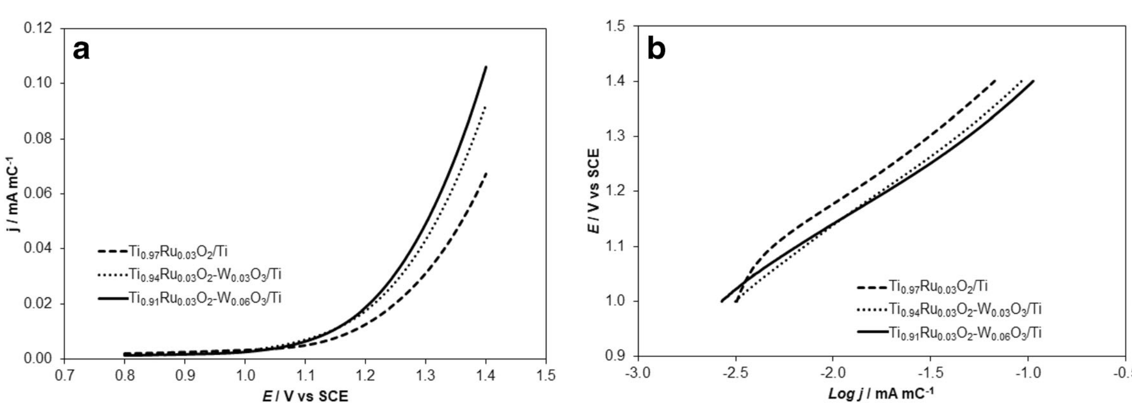

Fig. 6 Anodic polarization curves (**a**) and Tafel curves (**b**) recorded at $Ti_{0.97-x}Ru_{0.03}O_2$-W_xO_3/Ti electrodes in 0.1 M Na_2SO_4; $v = 5$ mV s^{-1}

Mineralisation of the dye solution observed as a decrease in TOC value can be observed at higher potentials at which other reactive oxygen species can be formed.

Corrosion Properties

The stability of the oxide electrodes, applied in processes of electrochemical oxidation of organic pollutants present in industrial wastewater, is very important. RuO_2 plays significant role in stability of $Ti_xRu_{1-x}O_2$/Ti electrodes because it undergoes serious corrosion in the oxygen evolution reaction. The stability of $Ti_xRu_{1-x}O_2$/Ti electrodes can be attributed to reactions of RuO_2 dissolution [20, 44]. The rate determining step includes the following reaction:

$$RuO_2 + H_2O \rightarrow RuO_2\text{–}OH + H^+ + e^- \quad (2)$$

The tested electrodes are characterized by relatively low amount of RuO_2 (3%) in the oxide layer on the electrode surface. Thus, it can be predicted that their corrosion can result from the formation of an interlayer of passivation on the substrate much more than from RuO_2 dissolution. Taking into consideration that products of the metal oxide degradation are soluble, the oxide film layer can be gradually enriched by insulating TiO_2 [57]. The electrode passivation results from application of TiO_2 as a stabilizing component of the oxide layer and TiO_2 comes from the titanium substrate.

Taking into consideration the lower content of RuO_2 (3%) and the higher content of TiO_2 (91–97%), it was necessary to determine the corrosion resistance of the tested electrodes and effect of WO_3 used in their modification. In order to assess an electrode stability, first of all, determination of the open circuit potential (OCP) was performed in the solution of 0.1 M Na_2SO_4. The obtained OCP values were 0.216 V ($Ti_{0.97}Ru_{0.03}O_2$/Ti), 0.226 V ($Ti_{0.94}Ru_{0.03}O_2$-$W_{0.03}O_3$/Ti) and 0.210 V ($Ti_{0.91}Ru_{0.03}O_2$-$W_{0.06}O_3$/Ti). Introduction of WO_3 into the oxide layer on the electrode surface does not change OCP value significantly and does not result in significant change in the electrode stability. In the case of $Ti_{0.7}Ru_{0.3}O_2$/Ti electrodes, their modification with WO_3 increased the OCP value by about 200 mV what meant higher stability of the modified electrodes attributed to domination of W species in the surface equilibria [44].

The corrosion of the tested electrodes was evaluated using potentiodynamic polarization sweep preceded by OCP determination. After the equilibrium was established, the polarization curves were recorded with the scan rate of 2 mV s^{-1}. The measurements were performed also at different immersion times (2 and 4 h) in 0.1 M Na_2SO_4. The representative polarization curves are shown in Fig. 7. The measured currents presented in the polarization curves were normalized with the respect to outer charge determined for the tested electrodes (Table 3) in order to take into consideration the change in the amount of the active sites on the electrode surface caused by the modification with WO_3.

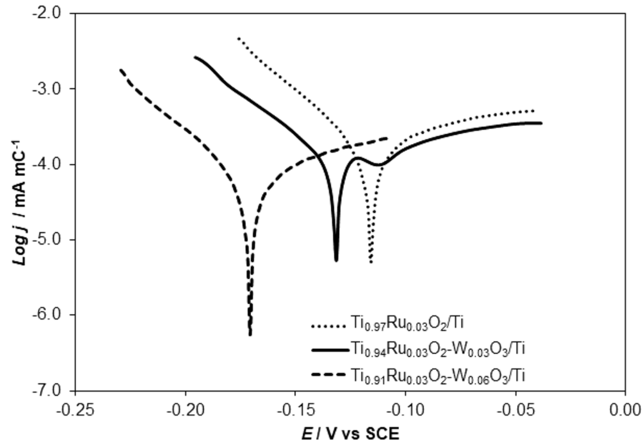

Fig. 7 Polarization curves measured for $Ti_{0.97\text{-}x}Ru_{0.03}O_2$-$W_xO_3$/Ti electrodes after 2-h immersion in Na_2SO_4 solution

The electrochemical parameters: anodic and cathodic Tafel slopes (b_a and b_c), corrosion current density (j_{corr}) and corrosion potential (E_{corr}), determined from the polarization curves are presented in Tables 4 and 5. Corrosion current density was calculated with the respect to the outer charge determined for the tested electrodes (Table 3).

The lowest value of E_{corr} determined from polarization curves recorded during the first measurement (Table 4) was observed for $Ti_{0.91}Ru_{0.03}O_2$-$W_{0.06}O_3$/Ti electrode in comparison with $Ti_{0.94}Ru_{0.03}O_2$-$W_{0.03}O_3$/Ti and $Ti_{0.97}Ru_{0.03}O_2$/Ti electrodes. Introduction of 3% WO_3 did not change E_{corr} value, but in the case of 6% WO_3 addition, E_{corr} was lower by almost 30 mV. Taking into consideration that the corrosion potential is a thermodynamic parameter and determines corrosion tendency, it can be concluded that modification of the electrodes with higher amount of WO_3 (6%) results in lower resistance to corrosion than in the case of the non-modified electrode. On the other hand, j_{corr} is a kinetic parameter which determines the corrosion rate. The lowest j_{corr} value determined from polarization curves recorded during the first measurement (Table 4) was observed in the case of the modified electrode with 6% WO_3—lower by 35% in comparison with the non-modified electrode. However, introduction of 3% WO_3 into the oxide film on the electrode surface resulted in slight increase (by 12%) in j_{corr}. Similar measurements were performed at different immersion times in Na_2SO_4 solution, and their results were compared with the corrosion parameters determined in the first measurement. The cathodic and anodic slopes determined for the tested electrodes immersed in Na_2SO_4 solution were almost independent on the immersion time and comparable for all tested electrodes (Table 5).

This means that the corrosion mechanism did not vary for $Ti_{0.97\text{-}x}Ru_{0.03}O_2$-$W_xO_3$/Ti electrodes even after 4-h

Table 4 Comparison of corrosion parameters determined from the polarization curves recorded during measurements after 2- and 4-h immersion in Na_2SO_4 solution

Electrode	Immersion time (h)	E_{corr} (V) vs. SCE	j_{corr} (mA mC^{-1})
$Ti_{0.97}Ru_{0.03}O_2$/Ti	0	− 0.018	6.90×10^{-5}
	2	− 0.116	9.44×10^{-5}
	4	− 0.126	11.55×10^{-5}
$Ti_{0.94}Ru_{0.03}O_2$-$W_{0.03}O_3$/Ti	0	− 0.018	7.72×10^{-5}
	2	− 0.132	7.10×10^{-5}
	4	− 0.206	6.17×10^{-5}
$Ti_{0.91}Ru_{0.03}O_2$-$W_{0.06}O_3$/Ti	0	− 0.046	4.49×10^{-5}
	2	− 0.170	4.48×10^{-5}
	4	− 0.251	4.49×10^{-5}

immersion. However, changes in E_{corr} values were clear (Table 4). In the case of all tested electrodes, E_{corr} shifted towards more negative potentials with increasing immersion time which proves less resistance to corrosion phenomena. The non-modified electrode revealed E_{corr} value lower by 98 mV, while the modified electrodes were characterized by E_{corr} value lower by 188 mV (3% WO_3) and 233 mV (6% WO_3) after 4-h immersion. The differences between E_{corr} determined for the tested electrodes immersed in Na_2SO_4 solution for 4 h prove that the electrodes modified with WO_3 became less resistant to corrosion in comparison with the non-modified one. On the other hand, the comparison of the corrosion current density determined for different immersion times (Table 4) was interesting. In the case of $Ti_{0.97}Ru_{0.03}O_2$/Ti electrode, the increase in immersion time resulted in an increase in j_{corr} by 67% (4 h). The electrode modified with 3% WO_3 revealed a decrease in j_{corr} by 20% after the 4-h immersion while j_{corr} values determined for the electrode modified with 6% WO_3 were independent on the immersion time. Comparison of j_{corr} values determined after the 4-h immersion resulted in the conclusion that the introduction of WO_3 into the oxide film at the electrode surface resulted in a decrease of j_{corr} by 47% (3% WO_3) and 61% (6% WO_3) in comparison with the non-modified electrode. This proves that the electrode modification with WO_3 results in lower corrosion rate which does not increase while the electrode is immersed in Na_2SO_4 solution. The higher amount of WO_3 in the oxide layer on electrode surface seems to be more advantageous.

Table 5 The mean values of Tafel slopes (anodic—b_a and cathodic—b_c) determined for $Ti_{0.97-x}Ru_{0.03}O_2$-W_xO_3/Ti electrodes immersed in Na_2SO_4 solution

Electrode	b_a (V dec^{-1})	b_c (V dec^{-1})
$Ti_{0.97}Ru_{0.03}O_2$/Ti	0.048	0.034
$Ti_{0.94}Ru_{0.03}O_2$-$W_{0.03}O_3$/Ti	0.045	0.033
$Ti_{0.91}Ru_{0.03}O_2$-$W_{0.06}O_3$/Ti	0.050	0.030

Accelerated Stability Tests

Stability of electrode material is very important in the process of organics degradation in wastewater. Thus, accelerated stability tests (ASTs) were performed under similar conditions as it was described in the case of $Ti_{0.7}Ru_{0.3}O_2$/Ti electrodes modified with 3 and 6% WO_3 [44]. The results of AST for $Ti_{0.97}Ru_{0.03}O_2$/Ti electrodes modified with 3 and 6% WO_3 are presented in Fig. 8.

In the beginning of the AST, the potential recorded for all tested electrodes decreased by 0.13 V during first 300 s. The decrease can be attributed to wetting of inner and less accessible surface of the tested electrodes [10]. This step was almost 5 times shorter than it was observed in the case of the $Ti_{0.7}Ru_{0.3}O_2$/Ti electrodes modified with 3 and 6% WO_3 [44], and can be explained by lower porosity of the tested electrodes. Afterward, clear increase in the potential was observed except for $Ti_{0.91}Ru_{0.03}O_2$-$W_{0.06}O_3$/Ti electrode which potential increased much slower. However, the final significant increase in the potential, indicating quick deactivation, was observed at clearly lower times than in the case of $Ti_{0.7}Ru_{0.3}O_2$/Ti electrodes modified with 3 and 6% WO_3 [44]. The lifetimes determined for the anodic potential of

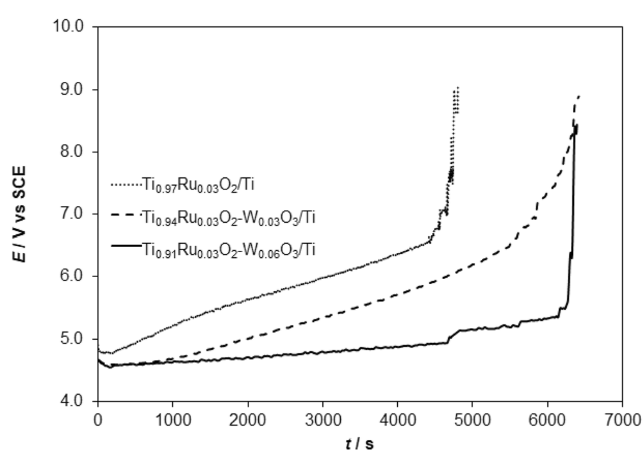

Fig. 8 Potential variation vs. time in ASTs for $Ti_{0.97-x}Ru_{0.03}O_2$-W_xO_3/Ti electrodes, recorded at 0.2 A cm^{-2} in 0.1 M Na_2SO_4

2 V higher than the potential at the time zero, were 1.27 h ($Ti_{0.97}Ru_{0.03}O_2/Ti$), 1.55 h ($Ti_{0.94}Ru_{0.03}O_2$-$W_{0.03}O_3/Ti$) and 1.76 h ($Ti_{0.91}Ru_{0.03}O_2$-$W_{0.06}O_3/Ti$). The modification of the electrodes with WO_3 results in their higher lifetime. However, lower content of RuO_2 (3%) in comparison with the electrodes containing 30% RuO_2 in the oxide film has significant effect on the electrode lifetime which is about 6 times lower.

The introduction of WO_3 into the oxide layer of $Ti_{0.97}Ru_{0.03}O_2/Ti$ electrodes seems to be advantageous taking into consideration their stability. One of possible reasons of electrode deactivation can be attributed to formation of insulating TiO_x interlayer [10, 58]. In comparison with $Ti_{0.97}Ru_{0.03}O_2/Ti$ electrode, the electrodes modified with WO_3 reveal less cracked structure (Fig. 5) which might result in retardancy of the electrolyte penetration into the surface of the substrate resulting and in a delay in the formation of insulating TiO_2 interlayer. The results prove that introduction of WO_3 into the oxide layer can improve the stability of $Ti_{0.97}Ru_{0.03}O_2/Ti$ electrode. Moreover, the higher content of WO_3 results in higher electrode lifetime. This also evidences the higher corrosion resistance of the modified electrodes, in Na_2SO_4 solution.

Conclusions

The $Ti_{0.97}Ru_{0.03}O_2/Ti$ electrodes modified with WO_3 are characterized by relatively low content of RuO_2 which is an electrocatalyst and has influence on electrode stability. The introduction of WO_3 to the oxide layer resulted in higher values of I_{pa} and I_{pc} determined for the electrode reaction in $K_4[Fe(CN)_6]$ solution, which also became more reversible in comparison with the non-modified electrode. A kinetic contribution to the reaction control was proved beside diffusion control. Thus, EAS of the tested electrodes was not determined with the application of the Randles-Sevcik equation, although the higher EAS for the modified electrodes could be predicted taking into consideration the obtained results. EAS determination in Na_2SO_4 solution proved an increase in the number of active sites in the oxide film for the modified electrodes. These sites were located mainly (more than 80%) at the outer and more accessible surface.

The investigation of the tested electrodes at potentials at which oxygen evolution is observed allowed their classification in the following order showing an increase in their activity towards OER: $Ti_{0.97}Ru_{0.03}O_2/Ti < Ti_{0.94}Ru_{0.03}O_2$-$W_{0.03}O_3/Ti < Ti_{0.91}Ru_{0.03}O_2$-$W_{0.06}O_3/Ti$. The latter electrode was also characterized by clear enhancement in the efficiency of electrochemical and photoelectrochemical degradation of an azo dye calculated as a decrease in COD and TOC corresponding to the dye solution mineralisation, which was described in [24]. Significant mineralisation was achieved at the potentials at which other reactive oxygen species could be formed.

Although the electrode modification with WO_3 resulted in lower resistance to corrosion taking into consideration E_{corr} (thermodynamic parameter) values after the 4-h immersion, j_{corr} values were lower by 47% (3% WO_3) and 61% (6% WO_3) in comparison with the non-modified electrode, what indicates a lower corrosion rate. Accelerated stability tests confirmed purposefulness of the electrode modification with WO_3. A small addition of WO_3 increased the lifetime of $Ti_{0.97}Ru_{0.03}O_2/Ti$ electrode. However, the lifetimes of the tested electrodes were about 6 times lower in comparison with the lifetimes determined for $Ti_{0.7}Ru_{0.3}O_2/Ti$ electrodes modified with the same amount of WO_3. That can be attributed to the lower content of RuO_2 (only 3%) and easier formation of insulating TiO_x interlayer.

Summing up, the modification of $Ti_{0.97}Ru_{0.03}O_2/Ti$ electrodes with WO_3 seems to be advantageous taking into consideration their application in electrochemical and photoelectrochemical degradation of organic compounds, e.g. azo dyes. Even though these electrodes are characterized by lower stability and corrosion resistance than $Ti_{0.7-x}Ru_{0.3}O_2$-W_xO_3/Ti electrodes, $Ti_{0.91}Ru_{0.03}O_2$-$W_{0.06}O_3/Ti$ electrode enables higher efficiency of electrochemical and photoelectrochemical treatment of wastewater containing organic pollutants.

References

1. S. Cherevko, S. Geiger, O. Kasian, N. Kulyk, J-P. Grote, A. Savan, B.R. Shrestha, S. Merzlikin, B. Breitbach, A. Ludwig, K.J.J. Mayrhofer, Oxygen and hydrogen evolution reactions on Ru, RuO_2, Ir, and IrO_2 thin film electrodes in acidic and alkaline electrolytes: a comparative study on activity and stability. Catal. Today **262**, 170–180 (2016)
2. Y. Yao, G. Teng, Y. Yang, C. Huang, B. Liu, L. Guo, Electrochemical oxidation of acetamiprid using Yb-doped PbO_2 electrodes: electrode characterization, influencing factors and degradation pathways. Sep. Purif. Technol. **211**, 456–466 (2019)
3. F. Moradi, C. Dehghanian, Addition of IrO_2 to RuO_2+TiO_2 coated anodes and its effect on electrochemical performance of anodes in acid media. Prog. Nat. Sci. Mater. Int. **24**(2), 134–141 (2014)

4. J.-M. Hu, J.-Q. Zhang, H.-M. Meng, C.-N. Cao, Microstructure, electrochemical surface and electrocatalytic properties of IrO_2+ Ta_2O_5 oxide electrodes. J. Mater. Sci. **38**(4), 705–712 (2003)
5. A.T. Marshall, R.G. Haverkamp, Nanoparticles of IrO_2 or Sb-SnO_2 increase the performance of iridium oxide DSA electrodes. J. Mater. Sci. **47**(3), 1135–1141 (2012)
6. J.F. Carneiro, J.R. Silva, R.S. Rocha, J. Ribeiro, M.R.V. Lanza, Morphological and electrochemical characterization of Ti/ $M_xTi_ySn_zO_2$ (M = Ir or Ru) electrodes prepared by the polymeric precursor method. Adv. Chem. Eng. Sci. **6**(4), 364–378 (2016)
7. J.J.S. Teles, E.R. Faria, D.V. Franco, L.M. Da Silva, Inner and outer surface areas, electrochemical porosity, and morphology factor of mixed oxide-covered mesh electrodes with a nominal composition of MOME-$Sn_{0.5}Ir_xRu_{(0.5-x)}O_2$. Int. J. Electrochem. Sci. **12**, 1755–1773 (2017)
8. J.-Y. Lee, D.-K. Kang, K. Lee, D. Chang, An investigation on the electrochemical characteristic of Ta_2O_5-IrO_2 anodes for the application of electrolysis process. Mater. Sci. Appl. **2**(04), 237–243 (2011)
9. Y. Lai, Y. Li, L. Jiang, W. Xu, X. Lv, J. Li, Y. Liu, Electrochemical behaviours of co-deposited Pb/Pb-MnO_2 composite anode in sulfuric acid solution–Tafel and EIS investigations. J. Electroanal. Chem. **671**, 16–23 (2012)
10. F. Fathollahi, M. Javanbakht, M.R. Ganjali, P. Nourozi, Electrochemical investigation of $Ru_{0.3}Ti_{0.7}O_2$ and $Ir_{0.3}Ti_{0.7}O_2$ coated titanium anodes for oxygen production processes. Anal. Bioanal. Electrochem. **5**(6), 689–697 (2013)
11. S. Trassati, Electrocatalysis: understanding the success of DSA®. Electrochim. Acta **45**, 377–2385 (2000)
12. Y. Feng, L. Yang, J. Liu, B.E. Logan, Electrochemical technologies for wastewater treatment and resource reclamation. Environ. Sci. Water Res. Technol. **2**(5), 800–831 (2016)
13. S. Vahidhabanu, J.S. Abilash, S. Ananthakumar, B.B. Ramesh, Effect of ruthenium oxide/titanium mesh anode microstructure on electrooxidation of pharmaceutical effluent. Int. J. Waste Resour. **5**(4) (2015). https://doi.org/10.4172/2252-5211.1000191
14. M.J.R. Santos, M.C. Medeiros, T.M.B.F. Oliveira, C.C.O. Morais, S.E. Mazzetto, C.A. Martinez-Huitle, S.S.L. Castro, Electrooxidation of cardanol on mixed metal oxide (RuO_2-TiO_2 and IrO_2-RuO_2-TiO_2) coated titanium anodes: insights into recalcitrant phenolic compounds. Electrochim. Acta **212**, 95–101 (2016)
15. P.V. Nidheesh, M. Zhou, M.A. Oturan, An overview on the removal of synthetic dyes from water by electrochemical advanced oxidation processes. Chemosphere **197**, 210–227 (2018)
16. D. Rajkumar, J.G. Kim, Oxidation of various reactive dyes with in situ electro-generated active chlorine for textile dyeing industry wastewater treatment. J. Hazard. Mater. **136**(2), 203–212 (2006)
17. S. Chen, Y. Zheng, S. Wang, X. Chen, Ti/RuO_2-Sb_2O_5-SnO_2 electrodes for chlorine evolution from seawater. Chem. Eng. J. **172**(1), 47–51 (2011)
18. S. Neodo, D. Rosestolato, S. Ferro, A. De Battisti, On the electrolysis of dilute chloride solutions: Influence of the electrode material on Faradaic efficiency for active chlorine, chlorate and perchlorate. Electrochim. Acta **80**, 282–291 (2012)
19. L. Xu, Y. Xin, J. Wang, A comparative study on IrO_2-Ta_2O_5 coated titanium electrodes prepared with different methods. Electrochim. Acta **54**(6), 1820–1825 (2009)
20. V.V. Panić, B.Ž. Nikolić, Sol-gel prepared active ternary oxide coating on titanium in cathodic protection. J. Serb. Chem. Soc. **72**(12), 1393–1402 (2007)
21. H. Yan, X. Wang, M. Yao, X. Yao, Band structure design of semiconductors for enhanced photocatalytic activity: the case of TiO_2. Prog. Nat. Sci. Mater. Int. **23**(4), 402–407 (2013)
22. V. Binas, D. Venieri, D. Kotzias, G. Kiriakidis, Modified TiO_2 based photocatalysts for improved air and health quality. J. Mater. **3**, 3–16 (2017)
23. E. Kusmierek, Semiconductor Electrode Materials Applied in Photoelectrocatalytic Wastewater Treatment–an Overview. Catalysts **10**(4), 439 (2020)
24. E. Kusmierek, E. Chrzescijanska, Application of TiO_2-RuO_2/Ti electrodes modified with WO_3 in electro- and photoelectrochemical oxidation of Acid Orange 7 dye. J. Photochem. Photobiol. A **302**, 59–68 (2015)
25. G.G. Bessegato, T.T. Guaraldo, M.V.B. Zanoni, in *Modern Electrochemical Methods in Nano, Surface and Corrosion Science*, ed. by M. Aliokhazraei. Enhancement of photoelectrocatalysis efficiency by using nanostructure electrodes. Chapter 10 (IntechOpen, London, UK, 2014)
26. H. Zhang, G. Chen, D.W. Bahnemann, in *Electrochemistry for the Environment*, ed. by C. Comninellis, G. Chen. Environmental photo(electro)catalysis: fundamentals. Chapter 16 (Springer, Berlin/Heidelberg, Germany, 2010)
27. H. Zhang, G. Chen, D.W. Bahnemann, Photoelectrocatalytic materials for environmental applications. J. Mater. Chem. **19**(29), 5089–5121 (2009)
28. T.T. Guaraldo, V.R. Goncales, B.F. Silva, S.I.C. de Toressi, M.V.B. Zanoni, Hydrogen production and simultaneous photoelectrocatalytic pollutant oxidation using a TiO_2/WO_3 nanostructured photoanode under visible light irradiation. J. Electroanal. Chem. **765**, 188–196 (2016)
29. Y.M. Hunge, A.A. Yadav, B.M. Mohite, V.L. Mathe, C.H. Bhosale, Photoelectrocatalytic degradation of sugarcane factory wastewater using WO_3/ZnO thin films. J. Mater. Sci. Mater. Electron. **29**, 3808–3816 (2018)
30. F.M. Toma, J.K. Cooper, V. Kunzelmann, M.T. McDowell, J. Lu, D.M. Larson, N.J. Borys, C. Abelyan, J.W. Beeman, K.M. Yu, et al., Mechanistic insights into chemical and photochemical transformations of bismuth vanadate photoanodes. Nat. Commun. **7**(1), 12012 (2016)
31. Y.R. Smith, B. Sarma, S.K. Mohanty, M. Misra, Formation of TiO_2-WO_3 nanotubular composite via single-step anodization and its application in photoelectrochemical hydrogen generation. Electrochem. Commun. **19**, 131–134 (2012)
32. K.R. Reyes-Gil, D.B. Robinson, WO_3-enhanced TiO_2 nanotube photoanodes for solar water splitting with simultaneous wastewater treatment. Appl. Mater. Interfaces **5**(23), 12400–12410 (2013)
33. Y. Xin, M. Gao, Y. Wang, D. Ma, Photoelectrocatalytic degradation of 4-nonylphenol in water with WO_3/TiO_2 nanotube array photoelectrodes. Chem. Eng. J. **242**, 162–169 (2014)
34. Y.M. Hunge, M.A. Mahadik, A.V. Moholkar, C.H. Bhosale, Photoelectrocatalytic degradation of oxalic acid using WO_3 and stratified WO_3/TiO_2 photocatalysts under sunlight illumination. Ultrason. Sonochem. **35**(Pt A), 233–242 (2017)
35. C. Cuevas-Arteaga, O.D.E. Cuevas, I. Rosales, Synthesis of TiO_2 nanotubular arrays and their electrochemical and photoelectrochemical properties to determine their use in photodegradation processes. Chem. Phys. Lett. **721**, 129–140 (2019)
36. P. Liao, E.A. Carter, New concepts and modelling strategies to design and evaluate photo-electro-catalysts based on transition metal oxides. Chem. Soc. Rev. **42**(6), 2401–2422 (2013)
37. V.V. Gorodetskii, V.A. Nerbuchilov, Tantalum oxide effect on the surface structure and morphology of the IrO_2 and IrO_2+RuO_2+TiO_2 coatings and on the corrosion and electrochemical properties of anodes prepared from these. Russ. J. Electrochem. **43**(2), 223–228 (2007)
38. I. Taurino, S. Carrara, M. Giorcelli, A. Tagliaferro, G. De Micheli, Comparison of two different carbon nanotube -based surfaces with respect to potassium ferricyanide electrochemistry. Surf. Sci. **606**(3–4), 156–160 (2012)
39. S.P. Mundinamani, M.K. Rabinal, Cyclic voltammetric studies on the role of electrode, electrode surface modification and electrolyte

solution of an electrochemical cell. J. Appl. Chem. **7**(9), 45–52 (2014)

40. L.K. Xu, J.D. Scantlebury, A study on the deactivation of an IrO_2-Ta_2O_5 coated titanium anode. Corros. Sci. **45**(12), 2729–2740 (2003)
41. J. Cheng, H. Zhang, G. Chen, Y. Zhang, Study of $Ir_xRu_{1-x}O_2$ oxides as anodic electrocatalysts for solid polymer electrolyte water electrolysis. Electrochim. Acta **54**(26), 6250–6256 (2009)
42. V.V. Panić, T.R. Vidaković, A.B. Dekanski, V.B. Mišković-Stanković, B.Ž. Nikolić, Capacitive properties of RuO_2-coated titanium electrodes prepared by the alkoxide ink procedure. J. Electroanal. Chem. **609**(2), 120–128 (2007)
43. J. Aromaa, O. Forsén, Evaluation of the electrochemical activity of a Ti-RuO_2-TiO_2 permanent anode. Electrochim. Acta **51**(27), 6104–6110 (2006)
44. E. Kusmierek, Electrochemical and corrosion characterization of TiO_2-RuO_2/Ti electrodes modified with WO_3. Electrocatalysis **10**(5), 499–515 (2019)
45. A. Bard, L.R. Faulkner, Electrochemical methods. Fundamentals and Applications. 2nd edn. (Wiley, New York 2001)
46. S.N. Azizi, S. Ghasemi, E. Chiani, Nickel/mesoporous silica (SBA-15) modified electrode: an effective porous material for electrooxidation of methanol. Electrochim. Acta **88**, 463–472 (2013)
47. A. Velazquez-Palenzuela, F. Centellas, J.A. Garrido, C. Arias, R.M. Rodriguez, E. Brillas, P.-L. Cabot, Kinetic analysis of carbon monoxide and methanol oxidation on high performance carbon-supported Pt-Ru electrocatalyst for direct methanol fuel cells. J. Power Sources **196**(7), 3503–3512 (2011)
48. C. Jo, I. Hwang, J. Lee, C.W. Lee, S. Yoon, Investigation of pseudocapacitive charge-storage behaviour in highly conductive ordered mesoporous tungsten oxide electrodes. J. Phys. Chem. C **115**(23), 11880–11886 (2011)
49. D.V. Zhuzhel'skii, E.G. Tolstopyatova, N.E. Kondrat'eva, S.N. Eliseeva, V.V. Kondrat'eva, Effect of electrode material on electrodeposition of tungsten oxide. Russ. J. Appl. Chem. **92**(7), 1006–1012 (2019)
50. C.-C. Huang, W. Xing, S.-P. Zhuo, Capacitive performance of amorphous tungsten oxide prepared by microwave irradiation. Scripta Mater. **61**, 985–987 (2009)
51. J.C. Van Kerkhof, W. Olthuis, P. Bergveld, M. Bos, Tungsten trioxide (WO_3) as an actuator electrode material for ISFET-based coulometric sensor-actuator systems. Sensor. Actuat. B-Chem. **3**(2), 129–138 (1991)
52. D. Szymanska, I.A. Rutkowska, L. Adamczyk, S. Zoladek, P.J. Kulesza, Effective charge propagation and storage in hybrid films of tungsten oxide and poly(3,4-ethylenedioxythiophene). J. Solid State Electrochem. **14**(11), 2049–2056 (2010)
53. J. Gaudet, A.C. Tavares, S. Trasatti, D. Guay, Physicochemical characterization of mixed RuO_2-SnO_2 solid solutions. Chem. Mater. **17**, 1570–1579 (2005)
54. E. Guerrini, H. Chen, S. Trasatti, Oxygen evolution on aged IrO_x/Ti electrodes in alkaline solutions. J. Solid State Electrochem. **11**(7), 939–945 (2007)
55. J.-M. Hu, J.-Q. Zhang, C.-N. Cao, Oxygen evolution reaction on IrO_2-based DSA® type electrodes: kinetics analysis of Tafel lines and EIS. Int. J. Hydrog. Energy **29**(8), 791–797 (2004)
56. K.-W. Kim, E.-H. Lee, J.-S. Kim, K.-H. Shin, K.-H. Kim, Study on the electro-activity and non-stoichiometry of a Ru-based mixed oxide electrode. Electrochim. Acta **46**(6), 915–921 (2001)
57. V.V. Panić, A.B. Dekanski, V.B. Mišković-Stanković, S. Milonjić, B.Ž. Nikolić, Differences in the electrochemical behaviour of activated titanium anodes prepared by the sol-gel procedure. J. Serb. Chem. Soc. **75**(10), 1413–1420 (2010)
58. R.D. Coteiro, F.S. Teruel, J. Ribeiro, A.R. de Andrade, Effect of solvent on the preparation and characterization of DSA®-type anode containing RuO_2-TiO_2-SnO_2. J. Braz. Chem. Soc. **17**(4), 771–779 (2006)